Multifunctional cork – alkali-activated fly ash composites: a sustainable material to enhance buildings' energy and acoustic performance

Rui M. Novais [a,*], João Carvalheiras [a], Luciano Senff [b], Ana M. Lacasta [c], Inma R. Cantalapiedra [c], Jessica Giro-Paloma [d], Maria P. Seabra [a], João A. Labrincha [a]

[a] Department of Materials and Ceramic Engineering / CICECO-Aveiro Institute of Materials, University of Aveiro, Campus Universitário de Santiago, 3810-193 Aveiro, Portugal

[b] Department of Mobility Engineering, Federal University of Santa Catarina (UFSC), 89.219-600 Joinville, SC, Brazil

[c] Barcelona School of Building Construction, Universitat Politècnica de Catalunya, Av. Doctor Marañon 44, 08028 Barcelona, Spain

[d] Departament de Ciència de Materials | Química Física, Universitat de Barcelona, C/ Martí i Franquès 1, 08028, Barcelona, Spain

*Corresponding author: Tel.: +351234370371; fax: +351234370204

E-mail address: ruimnovais@ua.pt (Rui M. Novais)

Declarations of interest: none

1

Abstract

This work evaluates, for the first time, the possibility of producing multifunctional alkali-activated composites combining ultra-low density, low thermal conductivity, high acoustic absorption, and good moisture buffering capacity. The composites were prepared using cork as a lightweight aggregate. This novel material might promote energy savings and tackle the CO_2 emissions of the building sector, while simultaneously improve the comfort for inhabitants (e.g. humidity levels regulation and sound pollution reduction). The composites apparent density (as low as 168 kg/m^3) and thermal conductivity (as low as 68 mW/m K) are amongst the lowest ever reported for alkali-activated materials (AAM) composites and foams, while their sound absorption ability is comparable to the best performing AAM foams reported to date, but in addition these eco-friendly composites also show good ability to passively adjust the humidity levels inside buildings. The multifunctional properties shown by the cork – AAM composites set them apart from other conventional building materials and might contribute to the global sustainability of the construction sector.

Keywords: alkali activation; thermal and acoustic insulation; moisture buffer value; cork; composite.

1. Introduction

Climate change is the most critical concern of the millennium due to its major impact in the environment. To reverse the distressing scenario forecast for the next century [1] a huge global effort has to be made in order to tackle greenhouse gases emissions. Policy makers have finally set in December 2015 the first-ever universal, legally binding agreement to keep global average temperature rise well below 2 ºC above pre-industrial

levels. Considering that anthropogenic emissions of greenhouse gases are one of the major drivers for climate change [2], their reduction is not only mandatory, but might strongly contribute to maintain the average global temperature below the 2 ºC limit over the 21st century, this considering a 40 to 70% reduction in the global anthropogenic greenhouse gases emissions by 2050 compared to 2010 [3]. The building sector is a hugely contributor to CO_2 emissions (36% of the emissions in EU), and in addition it also consumes a massive amount of energy (40% of the energy consumption in EU) [4]. Therefore, buildings represent an opportunity to strongly reduce anthropogenic greenhouse gases emissions provided that smart, sustainable, and energy-saving materials are used in their construction/rehabilitation. Green buildings are a new paradigm in the construction sector and could be a vital tool to boost the sector's sustainability [5–9]. In this context, multifunctional building materials designed to provide a combination of properties that might ensure energy-savings, while simultaneously enhance the interior environment quality for inhabitants are of great demand [10–12].

Alkali-activated materials (AAM) have recently gained renewed attention as an alternative to Portland cement [13] due to their much lower CO_2 emissions [14], provided that appropriate mixture design is employed in their synthesis [15]. Low density AAM might be an innovative strategy to mitigate the energy consumption of buildings. These materials might also ensure performance and environmental advantages over common insulating materials (e.g. polystyrene and polyurethane foams) since they possess much higher thermal stability [16] and may be produced using mainly/solely industrial wastes as solid precursors [17,18] instead of non-renewable fossil fuels. One particularly interesting approach to produce lightweight

3

AAM is through the use of lightweight aggregates, especially if natural aggregates [19] are employed, instead of synthetic or non-renewable aggregates [20,21].

The potential of AAM as low thermal conductivity materials has been deeply considered and demonstrated [22–24]. However, other relevant properties for building materials, such as their acoustic absorption [25–27] and moisture storage/release capacity [28], have received much less attention. The present investigation intends to fill the knowledge gap regarding the possibility of designing multifunctional AAM composites combining lightness, thermal conductivity, and acoustic insulation, coupled with the ability to passively adjust the humidity levels inside buildings. This is the first ever study addressing the AAM composites mechanical, thermal, acoustic, and moisture buffer properties.

Cork is an exceptional material combining low density [29], high porosity, excellent thermal and acoustic insulation [30,31], which associated with its outstanding sustainability (e.g. it is harvested without damaging the oak tree) makes it the ideal aggregate in the production of lightweight AAM. Surprisingly, the use of cork to produce AAM composites is extremely uncommon, up to now, there are only three studies addressing this possibility [19,32,33]. In addition, the emphasis of two of these studies was on cork's mechanical reinforcement ability [32], and on their added-value to promote wastewater depollution when incorporated into a metakaolin-zeolite AAM composite [33]. Therefore, our previous study was the first to evaluate the feasibility of using cork as a lightweight aggregate to synthesise ultra-light cork-AAM composites [19]. However, this study only evaluated the specimens' thermal insulation and thermal stability properties, while their acoustic and moisture buffering properties were not considered. In this study, besides evaluating the specimen's thermal insulation properties, the acoustic and moisture buffer properties of the AAM composites were

also measured. Such kind of exhaustive evaluation considering the thermal and acoustic insulation properties, as well as the moisture buffering ability has never been done before, neither for cork-AAM composites nor for any kind of lightweight AAM composites (using natural or synthetic aggregates) or foams. Therefore, the present investigation builds on our previous work, being a significant and necessary step forward to demonstrate the multifunctional properties of cork-AAM composites. In addition, the main solid precursor used to synthesise the AAM is an industrial waste (biomass fly ash), currently disposed in landfills, while in our previous study a commercial aluminosilicate (e.g. metakaolin) was used [19]. This strategy, aligned with the circular economy concept, further decreases the carbon footprint and production cost of these AAM composites. The influence of cork incorporation content on the cork − alkali-activated fly ash composites' compressive and flexural strength, thermal conductivity, apparent density, sound absorption, and moisture buffer ability was evaluated.

2. Experimental Conditions

2.1. Materials

Black expanded cork granules having ~6 mm in size and 70 g/cm^3 apparent density were used as light aggregates [19]. This is a by-product generated by the cork industry during the second trituration of rejected cork slabs. This type of cork as selected due to its low economic value.

Biomass fly ash wastes, produced by a Portuguese pulp and paper industry, were used as the main aluminosilicate source, while smaller amounts of metakaolin (Argical™ M1200S, Univar) were employed to adjust the binder SiO_2/Al_2O_3 ratio, which is a key

parameter to be considered in AAM. A mixture of sodium silicate (Quimiamel, Portugal) having a silica modulus of 3.2 and 10 M sodium hydroxide solution (ACS reagent, 97%; Sigma Aldrich) was used to perform the chemical activation of the fly ash-metakaolin precursors.

2.2. Cork – AAM composites

The reference composition (prepared without adding cork) was selected following previous studies by the authors [34,35]. First the solid precursors (70 wt.% fly ash and 30 wt.% metakaolin) were mixed manually, and then the alkaline activating solution (prepared in advance) was added to this mixture (1:1 weight ratio) to synthesise the alkali-activated material. The mixture between the solid precursors and the alkaline activators was carried out by using an intensive mixer (KichenAid®), having a geometry in accordance with DIN 1164, coupled with a flat paddle. The production of the composites required an additional step in which the cork granules (amount depending on the composition) were added to the slurry and mechanically mixed during 120 s. Eight different compositions containing various amounts of black expanded cork granules (ranging from 45 to 90 vol.%.) were synthesised. After mixing, the samples were transferred to metallic containers, and then placed in an oven (40 ℃; 1 day). It should be noticed that no attempt was made to remove the entrapped air during mixing (e.g. vibrating table) considering that the aim of this study is the production of lightweight composites. After 24 h, the specimens were removed from the moulds, and cured at 23 ℃ till the 28th day.

2.3. Materials characterisation

Scanning electron microscopy (SEM - Hitachi SU 70; energy dispersion spectroscopy – EDS Bruker) was used to study the specimen's microstructure.

The flexural and compressive strength of the specimens (4 cm x 4 cm x 16 cm) was determined 28 days after their synthesis following the standard EN 1015-11:1999 [36], by using a Universal Testing Machine (Shimadzu AG-25 TA; 0.5 mm/min; three samples per batch).

Thermal conductivity was measured on cubic samples (4 cm x 4 cm x 4 cm) by using a heat flowmeter apparatus following standard ASTM C518-04. The specimen is placed in the middle of two parallel plates, and then a unidirectional heat flux across the sample is imposed by using heat flux transducers which establish a temperature gradient between the top and bottom plates, respectively set to 55 and 40 ºC. The apparent density of the various samples (cubic geometry) was calculated by considering the ratio between their mass and volume. Both the thermal conductivity and the apparent density tests were performed on samples cured for 28 days. Three samples per composition were measured.

The samples ability to absorb and release water upon exposure to daily/cyclic humidity fluctuations was measured following the Nordtest protocol [37] and using a climatic chamber (Fitoclima 300 EP10 from Aralab). The mass variation of cylindrical specimens (d = 119.3 ± 0.8 mm; height = 21 ± 1 mm) was measured, and then the samples' moisture buffer value (MBV) determined using the equation (1):

$$MBV = \frac{\Delta m}{A \times \Delta\%RH} \tag{1}$$

where Δm is the mass variation (g), A corresponds to the exposed surface of the specimen (m^2), and $\Delta\%RH$ is the amplitude of the relative humidity (RH) (%). Before the tests, the samples were pre-conditioned at 63% RH until reaching steady-state (i.e.

constant mass) according to the ISO standard [38]. Then, the humidity levels inside the climatic chamber fluctuated between 75% (8 h) and 33% (16 h) in line with the Nordtest protocol. The humidity fluctuations were imposed during 120 h in order to complete five absorption/desorption cycles. A constant temperature of 23 ℃ was used in all cycles. One sample per composition was measured.

Cylindrical specimens (d = 50 mm; height ~20 mm) were used to evaluate the acoustic properties of the composites, namely their sound adsorption coefficient. Measurements were performed in an impedance tube by following the standard protocol EN ISO 10534-2 [39]. The principle is based on the transfer function measurements between two microphones. The test method covers the use of a tube with internal diameter of 50 mm, a sound generator, two ¼" identical microphones and a digital frequency analysis system. The sound source is connected to one end of the tube and the sample is placed at the other end. The source generates a random signal with flat spectral density. The tube is sufficiently long for plane waves to be fully developed before reaching the test specimen. Acoustic pressures were measured at two positions of the tube near the sample by two microphones mounted at 5 cm distance between them. From that signals, the complex acoustic transfer function was determined for the frequencies in the range 400–3150 Hz. In order to account for variations between microphones, the transfer function was measured in the normal manner, and then physically switched the location of the microphones and measured again, obtaining a corrected transfer function. From that, the complex reflection coefficient, R and the normal incident sound absorption coefficient, $\alpha = 1 - |R^2|$, were calculated. Two replicas per composition were evaluated, and the average data corresponding to at least four runs is shown.

3. Results and discussion

3.1. Microstructural analysis and composites apparent density

Fig. 1 shows a digital photograph of the alkali-activated fly ash binder and the cork-containing composites. The photograph of the AAM reveals the presence of small rounded pores attributed to the air entrapped in the slurry during mixing. It should be highlighted that no attempt was made to remove the entrapped air during mixing, this considering the main goal of this study (e.g. production of lightweight building materials). Hence, the samples were not vibrated. Fig. 1 also shows that the distribution of the cork granules in the matrix is dependent on the amount of cork added to the mixture. For the lowest cork-containing composites (cork below 60 vol.%) segregation between the cork and the matrix takes place. This phenomenon is particularly relevant in the sample containing 45 vol.% cork, being less evident, but still visible in the bottom part of the samples, in the composition containing 60 vol.% cork. In all the other cork-containing composites, a proper homogeneous distribution of the aggregate in the matrix is observed.
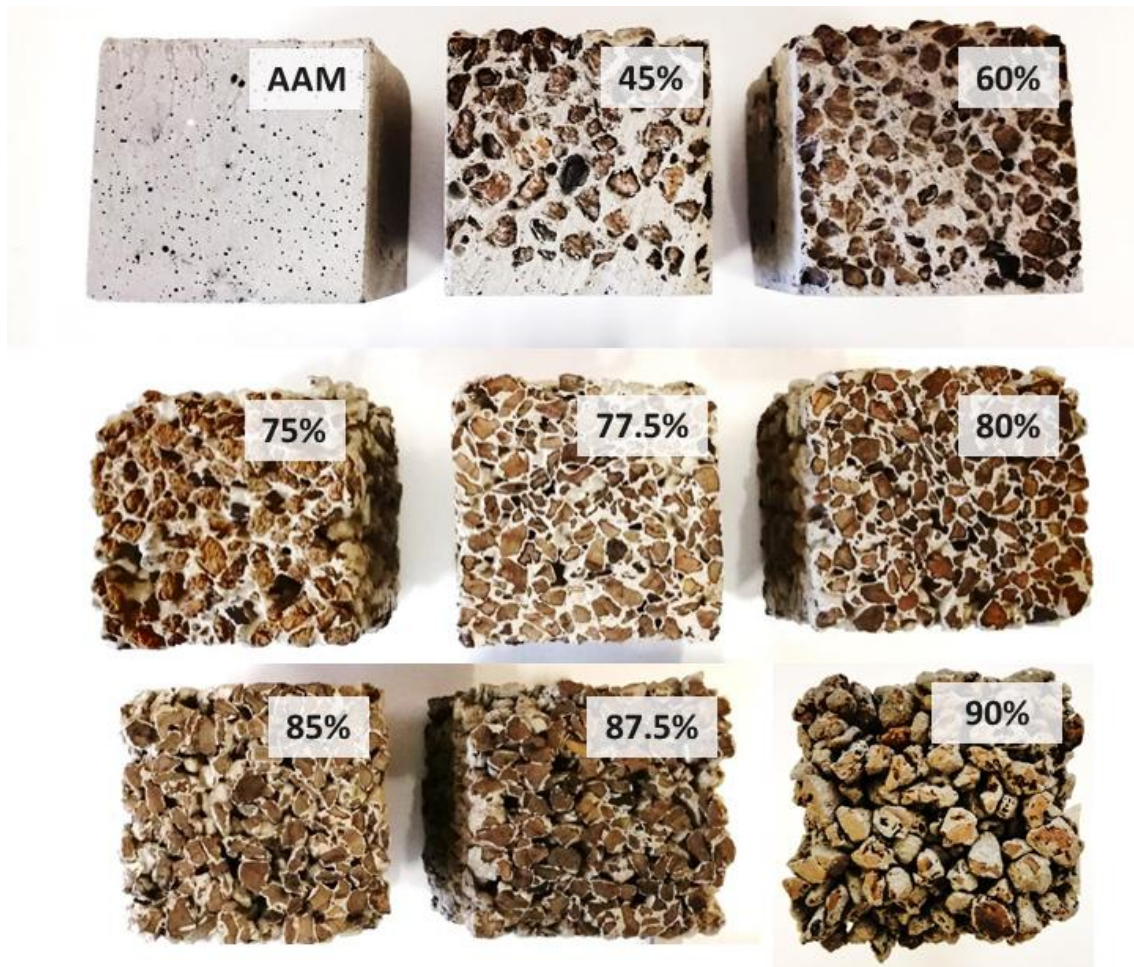
Fig. 1 Images of the alkali-activated fly ash composites containing various cork amounts (in vol.%).

While Fig. 2a presents a SEM micrograph of the AAM, Fig. 2b shows an EDS line profile, and Fig. 2 c-d present the EDS elemental mapping for Al, Si, Ca and Na. The EDS line profile shows a stable distribution of the selected elements (minor differences are attributed to topography), which is corroborated by the EDS elemental mapping (see Fig. 2d).
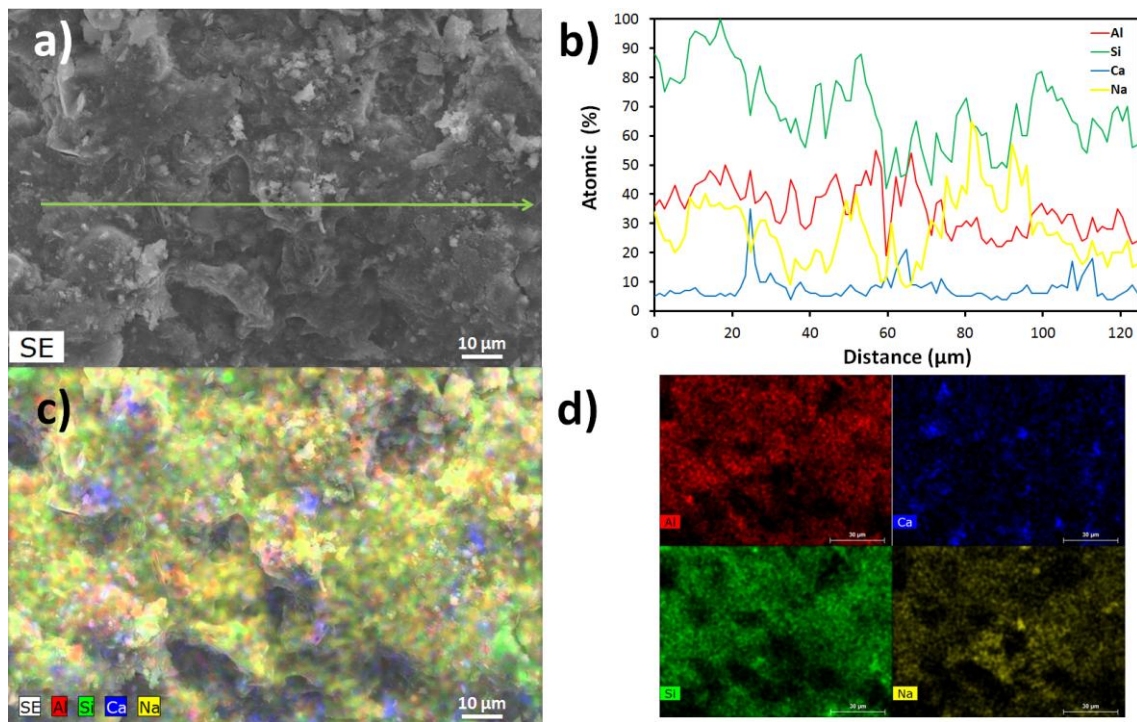
Fig. 2 SEM micrograph (a), EDS line profile (b) and elemental mapping (c and d) of the alkali-activated fly ash.

The interface between the matrix and the aggregate is very important and may strongly influence the mechanical properties and the durability of the produced composites [40]. Previous reports on AAM composites have shown the presence of voids, unreacted particles and cracks in the surrounding zone of the aggregates [41,42]. The interface between the aggregate (cork) and the matrix was studied using SEM and EDS line profile analysis, and results are shown in Fig. 3. The SEM micrograph does not show the presence of voids, neither cracks in the areas surrounding the aggregate. In addition, the EDS line profile shows that the chemical composition remains fairly stable in the matrix (see Fig. 3b), before changing at the vicinity of the interface. This remark is corroborated by the EDS elemental maps (shown in Fig. 3c and 3d) showing a homogeneous distribution of Si and Al in the matrix. These results are in line with our

previous work on cork- alkali activated metakaolin composites suggesting that the binder nature does not seem to affect the interface when cork is used as an aggregate [19]. Our results are also similar to other studies performed on AAM composites using limestone [43] and geopolymer aggregates [44]. Voids were not observed in these studies, still some cracks were seen, which were attributed to aggregates shrinkage [43,44].
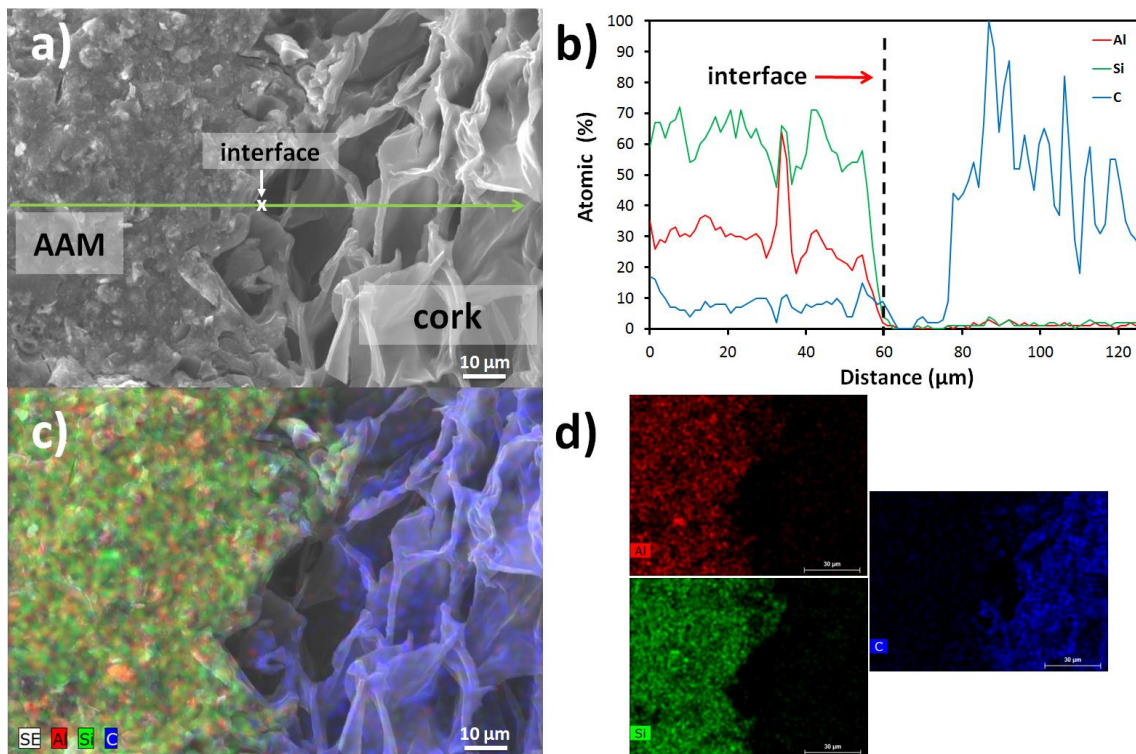

Fig. 3 SEM micrograph (a), EDS line profile (b) and elemental mapping (c and d) of the cork – alkali-activated composites containing 60 vol.% cork.

The incorporation of cork into the compositions promoted a significant decrease in their apparent density values, a sevenfold decrease from 1168 kg/m^3 (in the AAM) to 168 kg/m^3 (in the composite containing 90 vol.% cork) being observed, as shown in Fig. 4. Despite their extremely low apparent density it should be highlighted that this

composite (containing 90 vol.% cork) was mechanically very fragile. Nevertheless, the *in-situ* application of this composite would overcome their poor mechanical performance. On the contrary, the composite containing 87.5 wt.% can be easily handled, cut and transported without losing its integrity, enabling its pre-production as blocks.
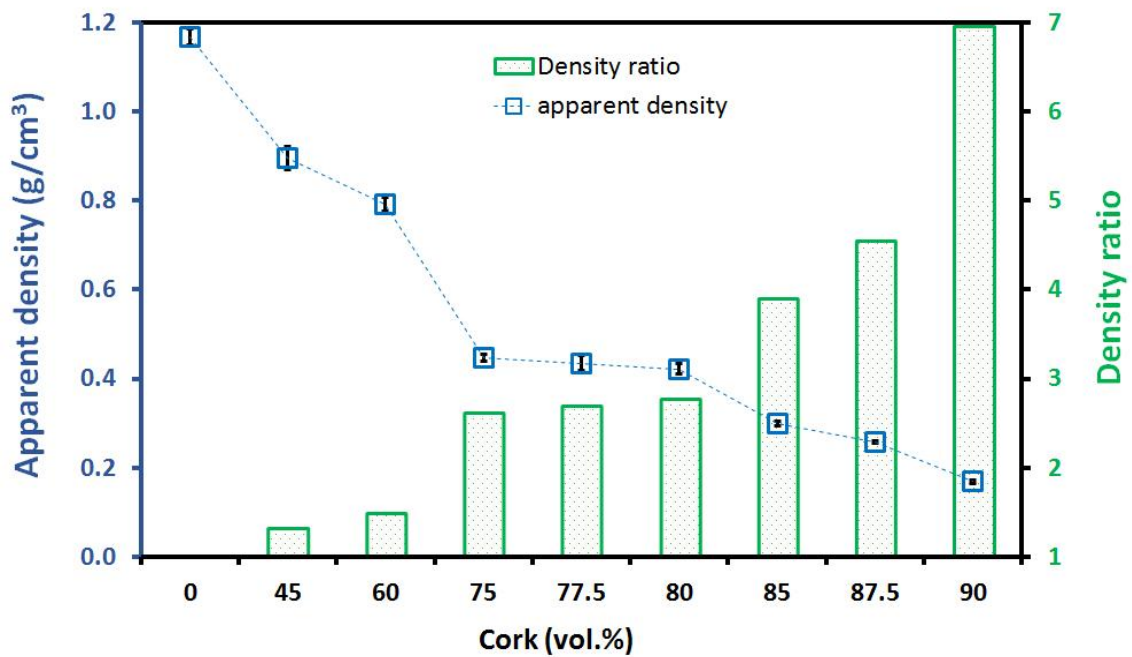

Fig. 4 Influence of the cork volume in the cork – alkali-activated composites apparent density (measured at the 28th day).

The lowest apparent densities here achieved (168 and 257 kg/m^3, for the 90 vol.% and the 87.5 vol.% cork containing composites, respectively) were compared with other published works on AAM composites and foams (prepared using foaming agents or surfactants), and results are presented in Table 1. This comparison shows that both specimens are amongst the lightest ever reported for AAM composites, being several times lower than those reported for expanded polystyrene (EPS) – AAM composites

(516 kg/m^3) [20], expanded glass – AAM composites (881 kg/m^3) [45], polyurethane – AAM composites (885 kg/m^3) [46], cenospheres – AAM composites (978 kg/m^3) [47], crumb rubber – AAM composites (1067 kg/m^3) [21], and expanded vermiculite – AAM composites (1918 kg/m^3) [48]; being only inferior to those of polystyrene – AAM composites (100 kg/m^3) [49]. Nevertheless, and despite the remarkable result reported by Duan *et al.* [49], these authors have used a non-sustainable aggregate (e.g. polystyrene) together with a foaming agent (3 wt.%), while in this study only cork, a natural and sustainable aggregate, was used. Hence, our approach might contribute to increase the sustainability of the construction sector.

Table 1 also shows that the lightest cork – AAM composite (90 vol.% cork) surpass all other reported values for AAM foams, including those of prepared with air entrapping agent [16], foaming agents (e.g. hydrogen peroxide [50–52], metallic powders [53,54] and protein-based [25]), and a mixture between foaming agents and surfactants [55–57]; being similar to the foam reported by Wu *et al.* (154 kg/m^3) [58]. These are very promising results, suggesting that the cork – AAM composites might be an excellent and environmentally friendlier alternative to AAM foams, particularly considering that the use of foaming agents at high dosages might jeopardize the AAM foams environmental benefits in comparison with Portland cement [59].

Table 2 presents the thermal conductivity of the AAM and the various cork – AAM composites. Not surprisingly, the thermal conductivity values significantly drop as the cork amount in the composites rise to 75 vol.%, but above this value much gentler thermal conductivity variation is seen as the cork content further rises. The lowest thermal conductivity value here achieved (68 mW/m K) was compared with other literature studies on AAM composites and foams, results being summarized in Fig. 5.
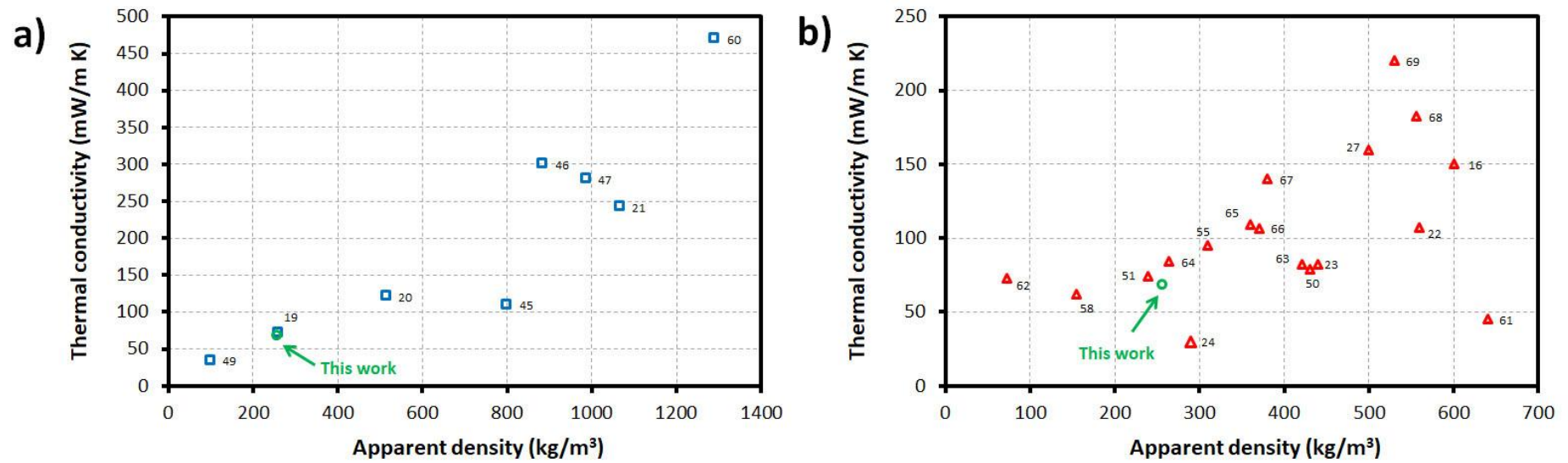
Fig. 5 Thermal conductivity of a) AAM composites made with various lightweight aggregates and b) AAM foams reported in literature. The lowest thermal conductivity value observed in this work was included in both charts for comparison (green circle).

Fig. 5a shows that the cork − AAM composite has the second lowest reported thermal conductivity for AAM composites, being several times inferior in comparison with the use of other lightweight aggregates: 6.9 times - oil palm shell [60]; 4.4 times − polyurethane [46]; 4.1 times − cenospheres [47]; 3.6 times − crumb rubber [21]; 1.8 times - polystyrene [20]; and 1.6 times − expanded glass [45]. To date, the lowest thermal conductivity for AAM composites has reported by Duan *et al.* (34 mW/m K) [49], this being half of value here reported, but achieved using a fossil fuel-derived aggregate (e.g. polystyrene) coupled with the addition of a significant amount of foaming agent (3 wt.%), while in this work only cork was used. In addition, the thermal conductivity of the cork − AAM composite is also comparable to the lowest values ever reported for AAM foams, as depicted from Fig. 5b. In fact, it is only higher than that reported in [24,61], being similar to [51,58,62], slightly inferior than [23,50,63,64], and much smaller than several other AAM foams (e.g. [65−69]). In addition, the thermal conductivity of the cork − AAM composite is also much lower than that reported for cork-containing Portland cement mortars (194.7 mW/m K) [70], including commercial products ((M150 − 209 mW/m K) [71], (137 mW/m K) [72]). These are very promising results demonstrating the outstanding potential of these cork − AAM composites as low thermal conductivity material.

3.2. Flexural and compressive strength measurements

The compressive and flexural strength of the matrix and the various cork-containing composites is shown in Fig. 6. The alkali-activated fly ash binder has a compressive strength of ~25 MPa and a flexural strength of ~4 MPa (at the 28th day). As expected, the cork − AAM composites show much lower strength values, this being particularly relevant in the highest containing cork composites. As mentioned in *section 3.1* the

16

composition containing 90 vol.% is very fragile, having 40 kPa in compressive strength. The composite containing 87.5 vol.% cork shows a ~4-fold increase in the compressive strength (150 kPa) and a ~5-fold increase in the flexural strength (120 kPa) in comparison with the composite containing 90 vol.% cork, in line with our previous remarks (see section 3.1). The compressive strength of this cork − AAM composite is superior to those of other low thermal conductivity materials, such as gypsum plaster-straw composite (4-71 kPa) [73] and EPS − Portland cement composites (80 kPa; 82.2 vol.% EPS) [74], while the compressive strength of the composite containing 80 vol.% cork (520 kPa) is superior to those of reported for AAM foams (e.g. 260 kPa [23], 200-400 kPa [75], 260 kPa; 230 kg/m^3 [76]).
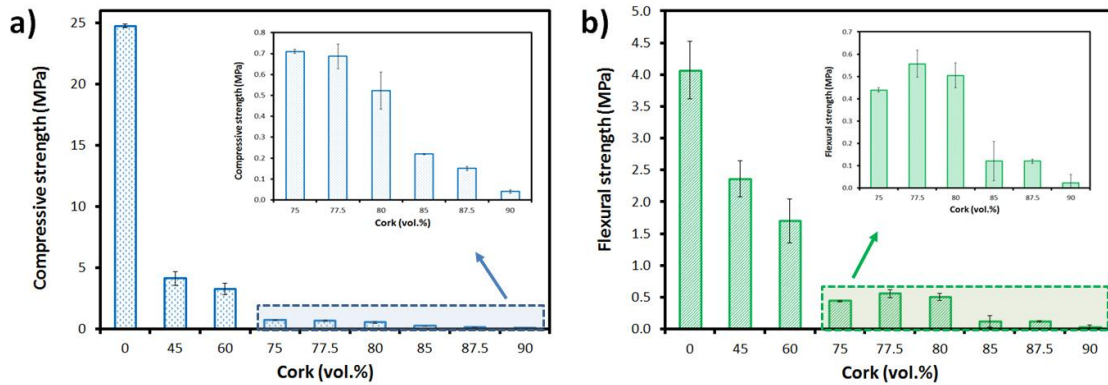

Fig. 6 a) Compressive and b) flexural strength of the various cork − alkali-activated composites. The insets in Fig. 3a and 3b better illustrate the mechanical performance of the cork − alkali-activated composites containing cork amounts higher than 75 vol.%.

3.3. Moisture buffer performance

The samples ability to store and release water when exposed to cyclic humidity fluctuations is shown in Fig. 7. Fig. 7a shows that the AAM has a pronounced tendency towards saturation. As observed, there is a continuous mass increase after each

adsorption/desorption cycle, meaning that the sample cannot efficiently desorb the water uptake in the previous step. This tendency in clearly illustrated by the dissimilar absorption and desorption rates presented in Fig. 8a. In any case, the practical MBV, shown in Fig. 8b, of the matrix is 0.89 g/m^2 $\Delta\%RH$. The cork – AAM composites showed a remarkably distinct behaviour, as seen by the mass evolution of these specimens upon humidity cycling. The lowest containing cork composite (45 vol.%) already shows an improved capacity to store and release water, see Fig. 7b, in comparison with the AAM (prepared without cork). Increasing the amount of cork in the composites to 75 vol.% strongly improves the samples absorption/desorption ability, and consequently the practical MBV rises from 1.37 (45 vol.%) to 1.89 g/m^2 $\Delta\%RH$ (75 vol.%). This corresponds to an impressive ~112% enhancement in the MBV in comparison with the matrix (0.89 g/m^2 $\Delta\%RH$), and demonstrates the feasibility of using cork – AAM composites as moisture regulators. In fact, according to the Nordtest protocol the MBV of this specimen is in the upper limit of the classification attributed to "good" moisture buffering materials (1.0<MBV<2.0 g/m^2 $\Delta\%RH$) [37], being very close to the best performing materials (MBV>2.0 g/m^2 $\Delta\%RH$; "Excelent").
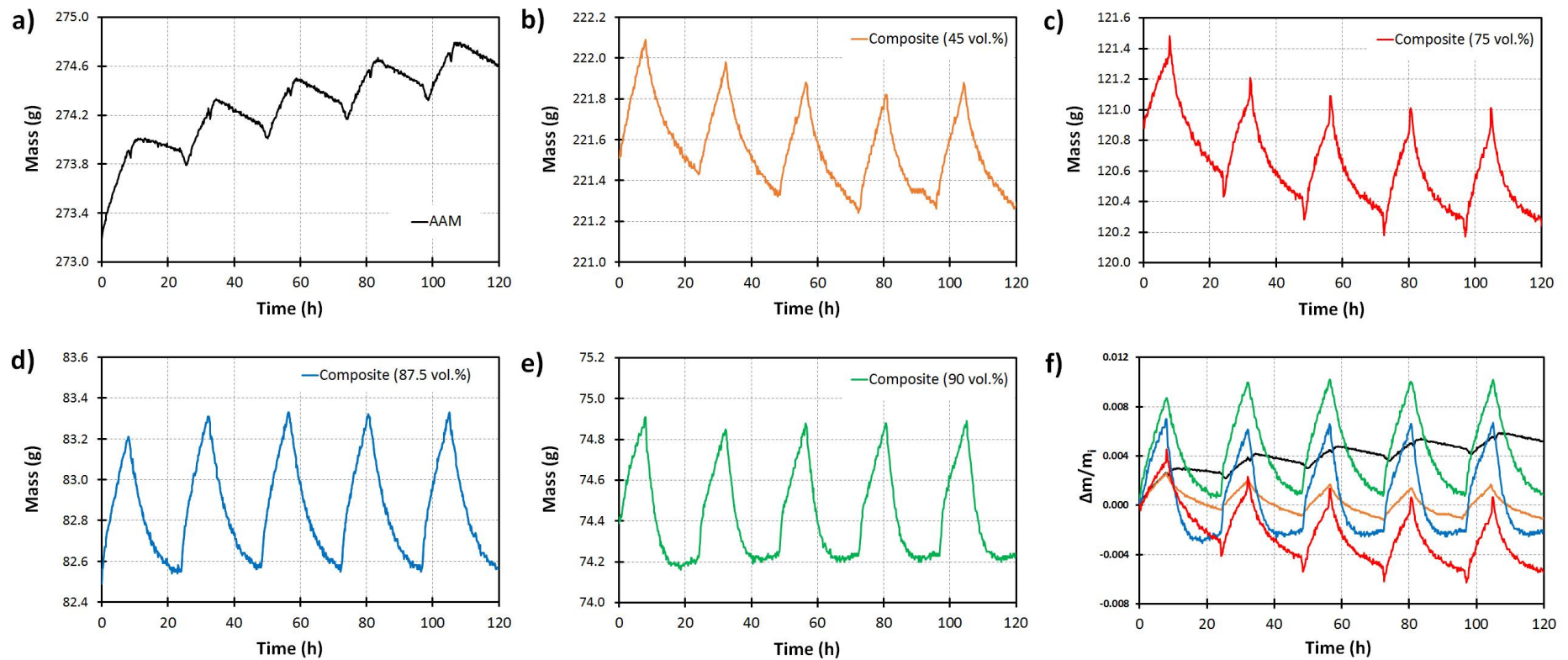
Fig. 7 Mass fluctuation of the alkali-activated fly ash (a) and the cork – alkali-activated composites (b-e) upon cyclic variation of the humidity, as prescribed by the Nordtest protocol [37]. Fig. 7f represents the ratio between the mass gradient and the specimens' initial mass.

Further rising the cork content to 87.5 vol.% does not improve the practical MBV, in fact a small decrease is observed (MBV = 1.64 g/m^2 $\Delta\%RH$). However, it does improve the stability of the absorption and desorption patterns, decreasing the differences between the absorption and desorption rates as seen in Fig. 8a. This is further illustrated in Fig. 7f, where the ratio between the mass gradient (Δm) and the specimens' initial mass (m$_i$) is presented for all samples. As shown, the composite containing 87.5 vol.% cork exhibits very reproducible absorption and desorption cycles demonstrating a good moisture buffering capacity. Increasing the cork content to 90 vol.% was detrimental to the practical MBV, which decreased to 1.46 g/m^2 $\Delta\%RH$. Nevertheless, the absorption and desorption pattern was reproducible and fairly stable throughout the five cycles (see Fig. 7e), showing once again that cork – AAM composites are very effective moisture regulators since they can absorb water when exposed to high humidity levels and then release it in equal amounts as the humidity level drops (see Fig. 7f and Fig. 8a). The ability of these cork – AAM composites to maintain steady absorption/desorption patterns upon cycling is a crucial technical advantage over other building materials (e.g. Portland-cement mortars [77,78] and AAM mortars [28]) envisioned for moisture buffering applications in which the specimens showed a tendency towards saturation suggesting that their performance in real environments could be compromised, or at least weakened, after a couple of cycles. To further demonstrate the performance stability of the AAM composites the number of absorption/desorption cycles were extended to 7 cycles, beyond those defined in the Nordtest protocol (5 cycles), and results are shown in Fig. S1 (as supplementary material). As observed, no significant changes occurred in neither of the samples: the mass of the matrix still increases after each cycle suggesting that this specimen will reach saturation, while the cork – AAM

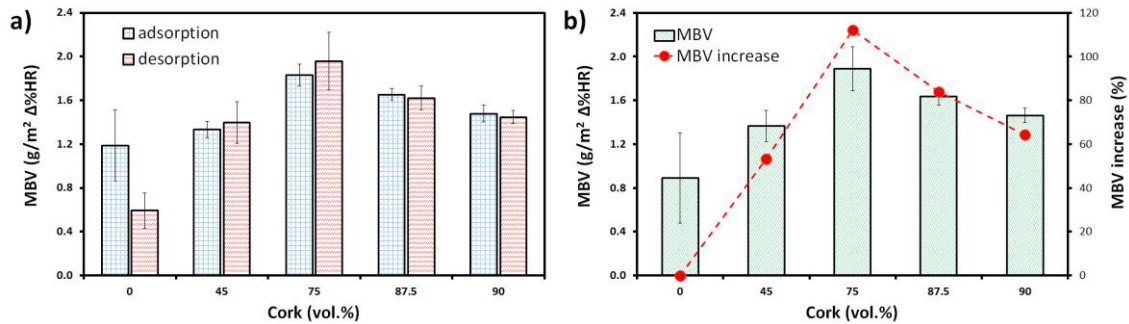composite shows an excellent capacity to absorb and release water upon daily cycling humidity fluctuation.

Fig. 8 a) Moisture buffer value determined from adsorption and desorption tests and b) practical MBV values for the AAM and the various cork – AAM composites.

The maximum practical MBV here achieved (1.89 g/m^2 $\Delta\%RH$) for the cork – AAM composites was compared with other literature studies, and results are shown in Fig. 9. It should be highlighted that up to now, there is only one other study focusing the moisture buffering ability of AAM and foamed AAM mortars [28], and for that reason Fig. 9 also contains values reported for other types of materials, such as Portland cement-mortars [77–80] and lime-based plaster [81]. De Rossi *et al.* [28] reported an MBV of 0.8 g/m^2 $\Delta\%RH$ for a alkali-activated fly ash mortar, this being similar to the value here achieved for the matrix (0.89 g/m^2 $\Delta\%RH$). These authors observed much higher MBVs, ranging from 4.03 to 5.61 g/m^2 $\Delta\%RH$ for the lightweight mortars, this being the highest value reported to date for binder materials. Nevertheless, and despite being remarkable results, their specimens showed a moderate tendency for saturation after each adsorption/desorption cycle, which could endanger the samples long-term performance. Fig. 9 also shows that besides these lightweight AAM mortars, there is

only one other binder material that surpasses the maximum MBV reached here, obtained with a Portland-cement mortar which was doped with a super absorbent polymer (2 wt.%) [77]. This mortar reached a practical MBV of 2.5 g/m^2 $\Delta\%RH$ with fairly stable adsorption and desorption pattern, even if a slight tendency for saturation was identified by the authors. The cork – AAM composites in this study surpass all other reported values for Portland cement mortars modified with vermiculite [77,78], perlite [77], cellulose [81], and super absorbent polymer [77–80], and also those reported for lime-based plaster [81]. These are very promising results demonstrating the interesting potential of these innovative materials as moisture buffer regulators. Moreover, our composites were produced using only cork which is a greener alternative to the use of super absorbent polymer or foaming agents. Nevertheless, the possibility of using minor amounts of foaming agents to further improve the cork – AAM composites cannot be ruled out, since it may strongly improve the moisture storage and release capacity of the specimens. This will be considered in future work.
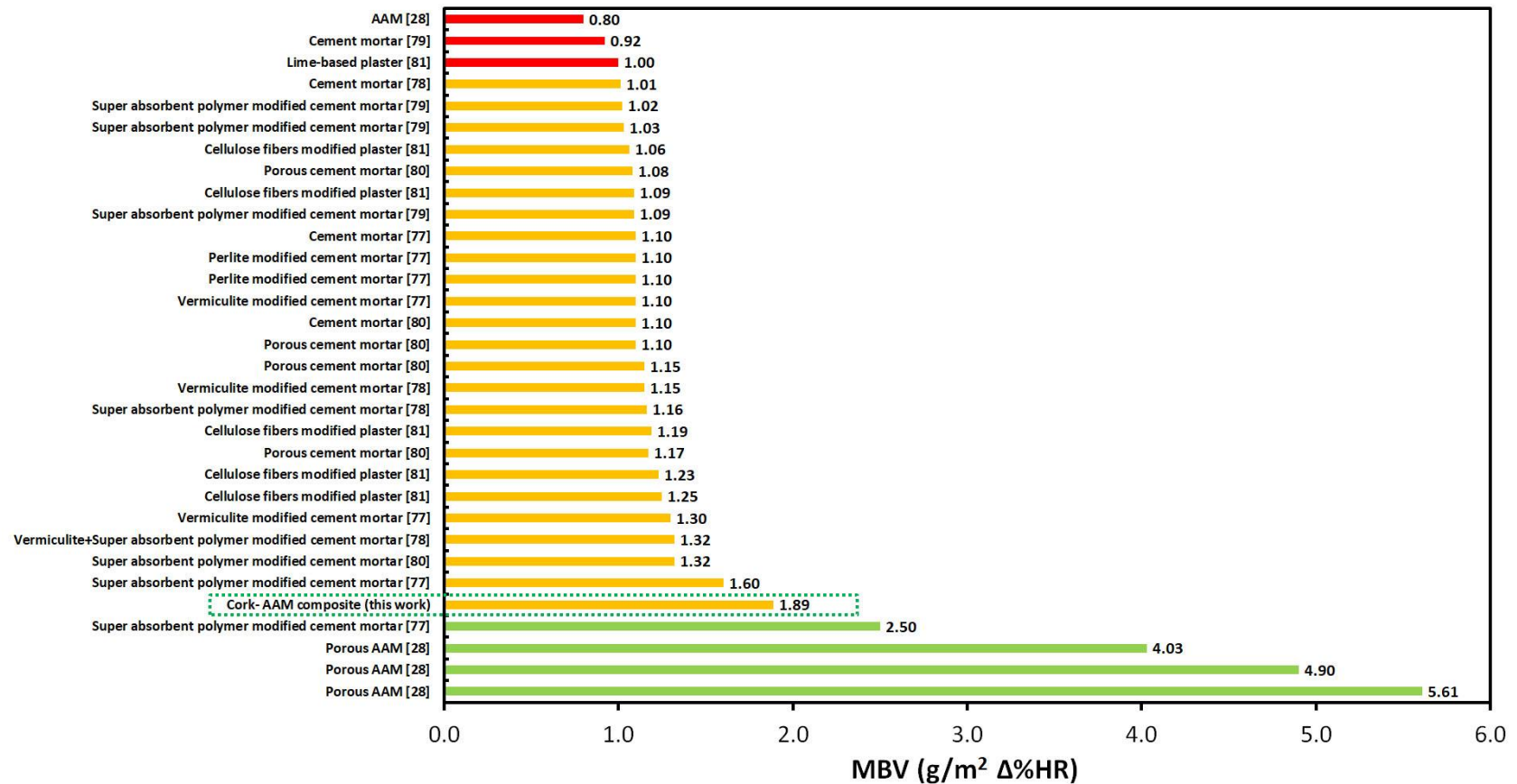
Fig. 9 Practical MBVs reported in literature for various building materials. The bars colour takes into accounts the MBV classes defined in the Nordtest protocol: red bars correspond to 0.5<MBV< 1.0 ("Moderate"), orange bars between 1.0<MBV< 2.0 ("Good") and green bars to MBV> 2.0 g/m^2 $\Delta\%RH$ ("Excellent").

3.4. Sound absorption

The sound absorption coefficient (α) of the matrix and the various cork – AAM composites across the frequency ranging from 400 to 3150 Hz is shown in Fig. 10.
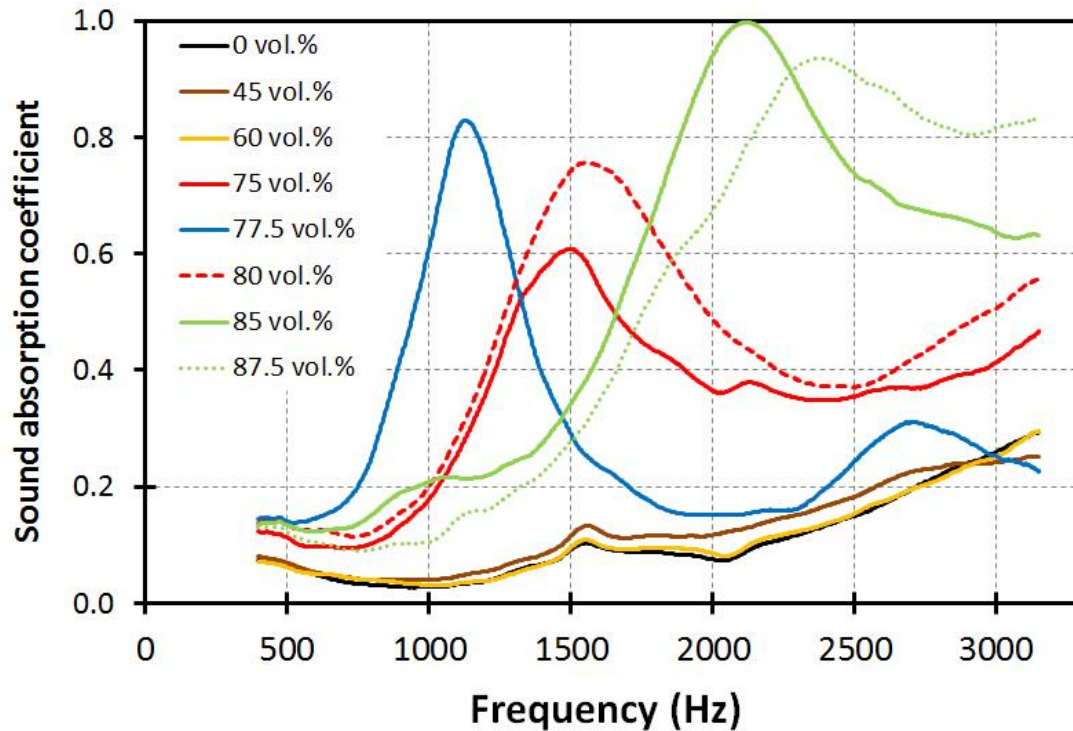

Fig. 10 Sound absorption coefficient measured for the AAM and the various cork – AAM composites.

As expected, the matrix shows a poor acoustic performance over this frequency range. Nevertheless, a slight increase in the sound absorption coefficient with increasing frequency was observed, reaching a $\alpha \sim 0.3$ in the high frequency range. The cork – AAM composites acoustic performance is highly dependent from the amount of cork added to the compositions. When the cork content is below 60 vol.% the absorption pattern is very similar to the one seen with the matrix, while above this threshold the sound absorption by the composites is impressively enhanced over the frequency range.

All composites (cork above 75 vol.%) show a very broad peak in the spectrum. However, the content of cork was found to affect not only the width and height of the peak, but also its location in the frequency range. In general, higher contents of cork improved the acoustic performance of the composites. The spectrum of the composite containing 75 vol.% cork shows a broad absorption peak between 1000 and 2000 Hz, in which the sound absorption coefficient ranges between 0.2 and 0.6. Above 2000 Hz and up to around 3000 Hz, α remains nearly constant, being always above 0.35. Higher amounts of cork further enhanced the composites sound absorption capacity, the best performing specimens being the ones having the higher amounts of cork (85 and 87.5 vol.%). The composite containing 85 vol.% of cork shows a remarkable absorption across the studied frequency range, but in particular beyond 1300 Hz. Above this frequency the sound absorption coefficient sharply increases reaching a stunning 100% sound absorption at ~2100 Hz ($\alpha = 1.0$). The composite containing 87.5 vol.% behaves similarly, however reaching a slightly lower α (0.94; ~2365 Hz). Nevertheless, the sound absorption of this composite is much greater in the high frequency range (> 2265 Hz), the absorption coefficient being always above 0.8, than the composite prepared with 87.5 vol.% in which α steadily decreases above 2265 Hz to ~0.63. These results show that cork incorporation in the compositions as a major effect in their sound absorption ability, this being one of the reasons we have decided to use it as a multifunctional aggregate in the production of eco-friendly building materials.

The sound acoustic performance of the cork − AAM composites is vastly superior to that reported for AAM foams [16,26,82]. Zhang *et al.* [16] reported very high sound absorption coefficient (0.7-1.0) but only in the low frequency range (from 40-150 Hz), while above this poor performance was seen (α not exceeding 0.3). The porous specimens reported by Luna-Galiano *et al.* [26] showed a distinct absorption pattern,

two distinct peaks being observed in the spectrum, one at low frequencies (~500 Hz) and another at around ~2500 Hz. However, their best performing foam had a maximum sound absorption coefficient of only ~0.25 (~2265 Hz) [26]. Recently, the same group have produced foams using an aluminium waste as a solid precursor and as a foaming agent [82]. Their specimens showed higher acoustic performance in comparison with their previous study [26]. In any case, the sound absorption coefficient of the best performing foam ranged between $0.15 < \alpha < 0.45$ (100-5000 Hz). Another study on AAM foams was recently reported by Stolz *et al.* [25]. Similar to that reported in [16], the foams showed high absorption at low frequency (α~0.85; 125-250 Hz), but then rapidly decreasing to ~0.15 in the range of 500-2000 Hz, before increasing again at higher frequencies (α below 0.55).

Our results can only be compared by those reported in [27,83,84]. Arenas *et al.* [84] prepared AAM mortars using coal fly ash as the solid precursor, and construction and demolition waste as aggregate. The mortar containing an aggregate:fly ash ratio of 80:20 showed a very interesting sound absorption capacity. Two major peaks were seen in the spectrum: one at 1000 Hz (α slightly below 0.9), and the second at 3000 Hz (α~0.65). Interesting results were also reported by Papa *et al.* by using silica-fume based foams [27]. The foams sound absorption was affected by the nature of the metakaolin and by the activating solution but ranged from 0.45-0.9 in the frequency ranges 1000-1500 Hz and 4200-6500 Hz. High sound absorption was also reported by Hung *et al.* when using a mixture of metakaolin and blast furnace slag, which were mixed with the alkaline solution and preformed air bubbles to produce lightweight AAM [83]. The lightest specimen (0.4 g/cm^3) showed very high α ranging from 0.5 (100 Hz) to 0.9 (4000 Hz). These results demonstrate that the cork – AAM composites show very interesting acoustic performance in comparison with all other published

literature on AAM. However, our best performing composite were produced using 87.5 vol.% of highly sustainable aggregate, without using foaming agents that could further boost the specimen's performance, which further demonstrate the potential of these innovative and eco-friendly composites.

4. Conclusions

This work evaluates, for the first time, the possibility of producing multifunctional cork-AAM composites exhibiting ultra-low density (as low as 168 kg/m^3), low thermal conductivity (as low as 68 mW/m K), high sound absorption coefficient (α = 1.0; ~2100 Hz) and good capacity to store and release water upon daily cyclic humidity fluctuations (maximum MBV = 1.89 g/m^2 $\Delta\%RH$). These remarkable properties, second lowest reported density and thermal conductivity for AAM composites, one of the best sound absorbent AAM, and its good moisture regulation ability, set them apart from other common building materials. The composites mechanical strength is modest (e.g. 150 kPa; 87.5 vol.% cork). However, it is still superior to those of other low thermal conductivity materials (e.g. gypsum plaster-straw composites and EPS-Portland cement composites).

Furthermore, the composites were produced using an exceptionally sustainable resource as aggregate (cork) and an industrial waste (biomass fly ash) as the main aluminosilicate source, this being a sustainable strategy aligned with the United Nations goals regarding the depletion of natural resources and promoting wastes valorisation.

Future work will evaluate the feasibility of using minor amounts of foaming agents in the compositions to further improve the cork – AAM composites' thermal, acoustic and moisture regulation ability.

References

[1] IPCC, Intergovernmental Panel on Climate Change Working Group I. Climate Change 2013: The Physical Science Basis. Long-term Climate Change: Projections, Commitments and Irreversibility, Cambridge Univ. Press. New York. (2013) 1029–1136. doi:10.1017/CBO9781107415324.024.

[2]   and P.Z. Blanco G., R. Gerlagh, S. Suh, J. Barrett, H. C. de Coninck, C. F. Diaz Morejon, R. Mathur, N. Nakicenovic, A. Ofosu Ahenkora, J. Pan, H. Pathak, J. Rice, R. Richels, S. J. Smith, D. I. Stern, F. L. Toth, Drivers, Trends and Mitigation. In: Climate Change 2014: Mitigation of Climate Change. Contribution of Working Group III to the Fifth Assessment Report of the Intergovernmental Panel on Climate Change, Cambridge Univ. Press. Cambridge, United Kingdom New York, NY, USA. (2014).

[3] L.A.M. and C.W.T. R.K. Pachauri, Climate Change 2014 Synthesis Report Summary Chapter for Policymakers, Ipcc. (2014) 151. doi:10.1017/CBO9781107415324.

[4] European Commission, (n.d.). https://ec.europa.eu/energy/en/topics/energy-efficiency/buildings (accessed July 10, 2019).

[5]   C. Zhang, C. Cui, Y. Zhang, J. Yuan, Y. Luo, W. Gang, A review of renewable energy assessment methods in green building and green neighborhood rating systems, Energy Build. 195 (2019) 68–81. doi:10.1016/j.enbuild.2019.04.040.

[6]   S. Yin, B. Li, Z. Xing, The governance mechanism of the building material industry (BMI) in transformation to green BMI: The perspective of green building, Sci. Total Environ. 677 (2019) 19–33. doi:10.1016/j.scitotenv.2019.04.317.

[7]   B.-J. He, Towards the next generation of green building for urban heat island mitigation: Zero UHI impact building, Sustain. Cities Soc. 50 (2019) 101647. doi:10.1016/j.scs.2019.101647.

[8]   J. Vieira, L. Senff, H. Gonçalves, L. Silva, V.M. Ferreira, J.A. Labrincha, Functionalization of mortars for controlling the indoor ambient of buildings, Energy Build. 70 (2014) 224–236. doi:10.1016/j.enbuild.2013.11.064.

[9]   A. Schackow, D. Stringari, L. Senff, S.L. Correia, A.M. Segadães, Influence of fired clay brick waste additions on the durability of mortars, Cem. Concr. Compos. 62 (2015) 82–89. doi:10.1016/j.cemconcomp.2015.04.019.

[10]   F. Barreca, V. Tirella, A self-built shelter in wood and agglomerated cork panels for temporary use in Mediterranean climate areas, Energy Build. 142 (2017) 1–7. doi:10.1016/j.enbuild.2017.03.003.

[11]   F. Barreca, C.R. Fichera, Thermal insulation performance assessment of agglomerated cork boards, Wood Fiber Sci. 48 (2016) 96–103.

[12]   F. Barreca, A. Martinez Gabarron, J.A. Flores Yepes, J.J. Pastor Pérez, Innovative use of giant reed and cork residues for panels of buildings in

Mediterranean area, Resour. Conserv. Recycl. 140 (2019) 259–266. doi:10.1016/j.resconrec.2018.10.005.

[13] J.L. Provis, Alkali-activated cementitious materials, Cem. Concr. Res. 114 (2018) 40–48. doi:10.1016/j.cemconres.2017.02.009.

[14] B.C. McLellan, R.P. Williams, J. Lay, A. Van Riessen, G.D. Corder, Costs and carbon emissions for geopolymer pastes in comparison to ordinary portland cement, J. Clean. Prod. 19 (2011) 1080–1090. doi:10.1016/j.jclepro.2011.02.010.

[15] L. Assi, K. Carter, E. (Eddie) Deaver, R. Anay, P. Ziehl, Sustainable concrete: Building a greener future, J. Clean. Prod. 198 (2018) 1641–1651. doi:10.1016/j.jclepro.2018.07.123.

[16] Z. Zhang, J.L. Provis, A. Reid, H. Wang, Mechanical, thermal insulation, thermal resistance and acoustic absorption properties of geopolymer foam concrete, Cem. Concr. Compos. 62 (2015) 97–105. doi:10.1016/j.cemconcomp.2015.03.013.

[17] R.M. Novais, J. Carvalheiras, M.P. Seabra, R.C. Pullar, J.A. Labrincha, Red mud-based inorganic polymer spheres bulk-type adsorbents and pH regulators, Mater. Today. xx (2019) 2017–2018. doi:10.1016/j.mattod.2019.01.014.

[18] E. Kränzlein, H. Pöllmann, W. Krcmar, Metal powders as foaming agents in fly ash based geopolymer synthesis and their impact on the structure depending on the Na /Al ratio, Cem. Concr. Compos. 90 (2018) 161–168. doi:10.1016/j.cemconcomp.2018.02.009.

[19] R.M. Novais, L. Senff, J. Carvalheiras, M.P. Seabra, R.C. Pullar, J.A. Labrincha, Sustainable and efficient cork - inorganic polymer composites: An innovative and eco-friendly approach to produce ultra-lightweight and low thermal

conductivity materials, Cem. Concr. Compos. 97 (2018) 107–117. doi:10.1016/J.CEMCONCOMP.2018.12.024.

[20] F. Colangelo, G. Roviello, L. Ricciotti, V. Ferrándiz-Mas, F. Messina, C. Ferone, O. Tarallo, R. Cioffi, C.R. Cheeseman, Mechanical and thermal properties of lightweight geopolymer composites, Cem. Concr. Compos. 86 (2018) 266–272. doi:10.1016/j.cemconcomp.2017.11.016.

[21] A. Wongsa, V. Sata, B. Nematollahi, J. Sanjayan, P. Chindaprasirt, Mechanical and thermal properties of lightweight geopolymer mortar incorporating crumb rubber, J. Clean. Prod. 195 (2018) 1069–1080. doi:10.1016/j.jclepro.2018.06.003.

[22] R.M. Novais, L.H. Buruberri, G. Ascensão, M.P. Seabra, J.A. Labrincha, Porous biomass fly ash-based geopolymers with tailored thermal conductivity, J. Clean. Prod. 119 (2016) 99–107. doi:10.1016/j.jclepro.2016.01.083.

[23] R.M. Novais, G. Ascensão, L.H. Buruberri, L. Senff, J.A. Labrincha, Influence of blowing agent on the fresh- and hardened-state properties of lightweight geopolymers, Mater. Des. 108 (2016) 551–559. doi:10.1016/j.matdes.2016.07.039.

[24] V. Vaou, D. Panias, Thermal insulating foamy geopolymers from perlite, Miner. Eng. 23 (2010) 1146–1151. doi:10.1016/j.mineng.2010.07.015.

[25] J. Stolz, Y. Boluk, V. Bindiganavile, Mechanical, thermal and acoustic properties of cellular alkali activated fly ash concrete, Cem. Concr. Compos. 94 (2018) 24–32. doi:10.1016/j.cemconcomp.2018.08.004.

[26] Y. Luna-Galiano, C. Leiva, C. Arenas, C. Fernández-Pereira, Fly ash based

geopolymeric foams using silica fume as pore generation agent. Physical, mechanical and acoustic properties, J. Non. Cryst. Solids. 500 (2018) 196–204. doi:10.1016/j.jnoncrysol.2018.07.069.

[27] E. Papa, V. Medri, D. Kpogbemabou, V. Morinière, J. Laumonier, A. Vaccari, S. Rossignol, Porosity and insulating properties of silica-fume based foams, Energy Build. 131 (2016) 223–232. doi:10.1016/j.enbuild.2016.09.031.

[28] R.F.P.M.M. A. De Rossi, J. Carvalheiras, R.M. Novais, M.J. Ribeiro, J.A. Labrincha, D. Hotza, Waste-based geopolymeric mortars with very high moisture buffering capacity, Constr. Build. Mater. 191 (2018) 39–46. doi:10.1016/j.conbuildmat.2018.09.201.

[29] R.M. Novais, R.C. Pullar, Comparison of low and high pressure infiltration regimes on the density and highly porous microstructure of ceria ecoceramics made from sustainable cork templates, J. Eur. Ceram. Soc. 39 (2019) 1287–1296. doi:10.1016/j.jeurceramsoc.2018.11.050.

[30] B. Abu-Jdayil, A.H. Mourad, W. Hittini, M. Hassan, S. Hameedi, Traditional, state-of-the-art and renewable thermal building insulation materials: An overview, Constr. Build. Mater. 214 (2019) 709–735. doi:10.1016/j.conbuildmat.2019.04.102.

[31] R. Maderuelo-Sanz, J.M. Barrigón Morillas, V. Gómez Escobar, Acoustical performance of loose cork granulates, Eur. J. Wood Wood Prod. 72 (2014) 321–330. doi:10.1007/s00107-014-0784-x.

[32] D.S. Roper, G.P. Kutyla, W.M. Kriven, Properties of cork particle reinforced sodium geopolymer composites, Ceram. Eng. Sci. Proc. 37 (2017) 79–82.

doi:10.1002/9781119321811.ch8.

[33] A. Sudagar, S. Andrejkovičová, C. Patinha, A. Velosa, A. McAdam, E.F. da Silva, F. Rocha, A novel study on the influence of cork waste residue on metakaolin-zeolite based geopolymers, Appl. Clay Sci. 152 (2018) 196–210. doi:10.1016/j.clay.2017.11.013.

[34] R.M. Novais, J. Carvalheiras, M.N. Capela, M.P. Seabra, R.C. Pullar, J.A. Labrincha, Incorporation of glass fibre fabrics waste into geopolymer matrices: An eco-friendly solution for off-cuts coming from wind turbine blade production, Constr. Build. Mater. 187 (2018) 876–883. doi:10.1016/j.conbuildmat.2018.08.004.

[35] M. Saeli, R.M. Novais, M.P. Seabra, J.A. Labrincha, Green geopolymeric concrete using grits for applications in construction, Mater. Lett. 233 (2018) 94–97. doi:10.1016/j.matlet.2018.08.102.

[36] E. 1015-11, Methods of test for mortar for masonry. Determination of flexural and compressive strength of hardened mortar, 1999.

[37] C. Rode, Moisture Buffering of Building Materials, Department of Civil Engineering Technical University of Denmark, 2005.

[38] I. 24353:2008 — H. performance of building materials and products: determination of moisture adsorption/desorption properties in response to Humidity, INTERNATIONAL STANDARD materials — Method for the determination, 2008 (2008).

[39] ISO 10534-2, Acoustics determination of sound absorption coefficient and impedance in impedance tubes - Part II: Transfer. Function. Method., (1998).

[40] R. San Nicolas, J.L. Provis, The Interfacial Transition Zone in Alkali-Activated Slag Mortars, Front. Mater. 2 (2015) 1–11. doi:10.3389/fmats.2015.00070.

[41] H. Peng, C. Cui, C.S. Cai, Y. Liu, Z. Liu, Microstructure and microhardness property of the interface between a metakaolin/GGBFS-based geopolymer paste and granite aggregate, Constr. Build. Mater. 221 (2019) 263–273. doi:10.1016/j.conbuildmat.2019.06.090.

[42] B. Singh, M.R. Rahman, R. Paswan, S.K. Bhattacharyya, Effect of activator concentration on the strength, ITZ and drying shrinkage of fly ash/slag geopolymer concrete, Constr. Build. Mater. 118 (2016) 171–179. doi:10.1016/j.conbuildmat.2016.05.008.

[43] F. Pacheco-Torgal, J. Castro-Gomes, S. Jalali, Investigations about the effect of aggregates on strength and microstructure of geopolymeric mine waste mud binders, Cem. Concr. Res. 37 (2007) 933–941. doi:10.1016/j.cemconres.2007.02.006.

[44] Yliniemi, Paiva, Ferreira, Tiainen, Illikainen, Development and incorporation of lightweight waste-based geopolymer aggregates in mortar and concrete, Constr. Build. Mater. 131 (2017) 784–792. doi:10.1016/j.conbuildmat.2016.11.017.

[45] D.M.A. Huiskes, A. Keulen, Q.L. Yu, H.J.H. Brouwers, Design and performance evaluation of ultra-lightweight geopolymer concrete, Mater. Des. 89 (2016) 516–526. doi:10.1016/j.matdes.2015.09.167.

[46] L. Bergamonti, R. Taurino, L. Cattani, D. Ferretti, F. Bondioli, Lightweight hybrid organic-inorganic geopolymers obtained using polyurethane waste, Constr. Build. Mater. 185 (2018) 285–292.

doi:10.1016/j.conbuildmat.2018.07.006.

[47]   A. Hajimohammadi, T. Ngo, J.L. Provis, T. Kim, J. Vongsvivut, High strength/density ratio in a syntactic foam made from one-part mix geopolymer and cenospheres, Compos. Part B Eng. 173 (2019) 106908. doi:10.1016/j.compositesb.2019.106908.

[48]   L. Zuda, J. Drchalová, P. Rovnaník, P. Bayer, Z. Keršner, R. Černý, Alkali-activated aluminosilicate composite with heat-resistant lightweight aggregates exposed to high temperatures: Mechanical and water transport properties, Cem. Concr. Compos. 32 (2010) 157–163. doi:10.1016/j.cemconcomp.2009.11.009.

[49]   P. Duan, L. Song, C. Yan, D. Ren, Z. Li, Novel thermal insulating and lightweight composites from metakaolin geopolymer and polystyrene particles, Ceram. Int. 43 (2017) 5115–5120. doi:10.1016/j.ceramint.2017.01.025.

[50]   R.M. Novais, G. Ascensão, D.M. Tobaldi, M.P. Seabra, J.A. Labrincha, Biomass fly ash geopolymer monoliths for effective methylene blue removal from wastewaters, J. Clean. Prod. 171 (2018) 783–794. doi:10.1016/j.jclepro.2017.10.078.

[51]   J. Feng, R. Zhang, L. Gong, Y. Li, W. Cao, X. Cheng, Development of porous fly ash-based geopolymer with low thermal conductivity, Mater. Des. 65 (2015) 529–533. doi:10.1016/j.matdes.2014.09.024.

[52]   R.M. Novais, L.H. Buruberri, M.P. Seabra, D. Bajare, J.A. Labrincha, Novel porous fly ash-containing geopolymers for pH buffering applications, J. Clean. Prod. 124 (2016) 395–404. doi:10.1016/j.jclepro.2016.02.114.

[53]   R.M. Novais, G. Ascensão, N. Ferreira, M.P. Seabra, J.A. Labrincha, Influence

of water and aluminium powder content on the properties of waste-containing geopolymer foams, Ceram. Int. 44 (2018) 6242–6249. doi:10.1016/j.ceramint.2018.01.009.

[54] W.D.A. Rickard, A. Van Riessen, Performance of solid and cellular structured fly ash geopolymers exposed to a simulated fire, Cem. Concr. Compos. 48 (2014) 75–82. doi:10.1016/j.cemconcomp.2013.09.002.

[55] Y. Cui, D. Wang, J. Zhao, D. Li, S. Ng, Y. Rui, Effect of calcium stearate based foam stabilizer on pore characteristics and thermal conductivity of geopolymer foam material, J. Build. Eng. 20 (2018) 21–29. doi:10.1016/j.jobe.2018.06.002.

[56] A. Hajimohammadi, T. Ngo, P. Mendis, Enhancing the strength of pre-made foams for foam concrete applications, Cem. Concr. Compos. 87 (2018) 164–171. doi:10.1016/j.cemconcomp.2017.12.014.

[57] L. Korat, V. Ducman, The influence of the stabilizing agent SDS on porosity development in alkali-activated fly-ash based foams, Cem. Concr. Compos. 80 (2017) 168–174. doi:10.1016/j.cemconcomp.2017.03.010.

[58] J. Wu, Z. Zhang, Y. Zhang, D. Li, Preparation and characterization of ultra-lightweight foamed geopolymer (UFG) based on fly ash-metakaolin blends, Constr. Build. Mater. 168 (2018) 771–779. doi:10.1016/j.conbuildmat.2018.02.097.

[59] Z. Zhang, J.L. Provis, A. Reid, H. Wang, Geopolymer foam concrete: An emerging material for sustainable construction, Constr. Build. Mater. 56 (2014) 113–127. doi:10.1016/j.conbuildmat.2014.01.081.

[60] M.Y.J. Liu, U.J. Alengaram, M.Z. Jumaat, K.H. Mo, Evaluation of thermal

conductivity, mechanical and transport properties of lightweight aggregate foamed geopolymer concrete, Energy Build. 72 (2014) 238–245. doi:10.1016/j.enbuild.2013.12.029.

[61]　H.S. Hassan, H.A. Abdel-Gawwad, S.R.V. García, I. Israde-Alcántara, Fabrication and characterization of thermally-insulating coconut ash-based geopolymer foam, Waste Manag. 80 (2018) 235–240. doi:10.1016/j.wasman.2018.09.022.

[62]　M. Lassinantti Gualtieri, M. Romagnoli, A.F. Gualtieri, Preparation of phosphoric acid-based geopolymer foams using limestone as pore forming agent - Thermal properties by in situ XRPD and Rietveld refinements, J. Eur. Ceram. Soc. 35 (2015) 3167–3178. doi:10.1016/j.jeurceramsoc.2015.04.030.

[63]　M. Łach, K. Korniejenko, J. Mikuła, Thermal Insulation and Thermally Resistant Materials Made of Geopolymer Foams, Procedia Eng. 151 (2016) 410–416. doi:10.1016/j.proeng.2016.07.350.

[64]　G. Samson, M. Cyr, X.X. Gao, Thermomechanical performance of blended metakaolin-GGBS alkali-activated foam concrete, Constr. Build. Mater. 157 (2017) 982–993. doi:10.1016/j.conbuildmat.2017.09.146.

[65]　P. Palmero, A. Formia, P. Antonaci, S. Brini, J.M. Tulliani, Geopolymer technology for application-oriented dense and lightened materials. Elaboration and characterization, Ceram. Int. 41 (2015) 12967–12979. doi:10.1016/j.ceramint.2015.06.140.

[66]　C. Bai, T. Ni, Q. Wang, H. Li, P. Colombo, Porosity, mechanical and insulating properties of geopolymer foams using vegetable oil as the stabilizing agent, J.

Eur. Ceram. Soc. 38 (2018) 799–805. doi:10.1016/j.jeurceramsoc.2017.09.021.

[67]   L. Dembovska, D. Bajare, V. Ducman, L. Korat, G. Bumanis, The use of different by-products in the production of lightweight alkali activated building materials, Constr. Build. Mater. 135 (2017) 315–322. doi:10.1016/j.conbuildmat.2017.01.005.

[68]   F. Xu, G. Gu, W. Zhang, H. Wang, X. Huang, J. Zhu, Pore structure analysis and properties evaluations of fly ash-based geopolymer foams by chemical foaming method, Ceram. Int. 44 (2018) 19989–19997. doi:10.1016/j.ceramint.2018.07.267.

[69]   E. Prud'homme, P. Michaud, E. Joussein, C. Peyratout, A. Smith, S. Arrii-Clacens, J.M. Clacens, S. Rossignol, Silica fume as porogent agent in geo-materials at low temperature, J. Eur. Ceram. Soc. 30 (2010) 1641–1648. doi:10.1016/j.jeurceramsoc.2010.01.014.

[70]   A. Moreira, J. António, A. Tadeu, Lightweight screed containing cork granules: Mechanical and hygrothermal characterization, Cem. Concr. Compos. 49 (2014) 1–8. doi:10.1016/j.cemconcomp.2014.01.012.

[71]   Technical properties of lightweight concrete with expanded cork granules. Amorim Isolamentos. Available from: https://www.amorimisolamentos.com/xms/files/FICHAS_TECNICAS_2017/Fichas_EN/lightweight_concrete_screed_filling.pdf. (Accessed 12 December 2019).

[72]   Ecocork floor (technical datasheet). Secil. Available from: https://www.secilargamassas.pt/uploads/documentos/Ficha_Tecnica_BETONILHA_ecoCORK.pdf. (Accessed 12 December 2019).

[73] N. Belayachi, D. Hoxha, M. Slaimia, Impact of accelerated climatic aging on the behavior of gypsum plaster-straw material for building thermal insulation, Constr. Build. Mater. 125 (2016) 912–918. doi:10.1016/j.conbuildmat.2016.08.120.

[74] A.A. Sayadi, J. V. Tapia, T.R. Neitzert, G.C. Clifton, Effects of expanded polystyrene (EPS) particles on fire resistance, thermal conductivity and compressive strength of foamed concrete, Constr. Build. Mater. 112 (2016) 716–724. doi:10.1016/j.conbuildmat.2016.02.218.

[75] M.S. Cilla, M.D. de Mello Innocentini, M.R. Morelli, P. Colombo, Geopolymer foams obtained by the saponification/peroxide/gelcasting combined route using different soap foam precursors, J. Am. Ceram. Soc. 100 (2017) 3440–3450. doi:10.1111/jace.14902.

[76] S. Petlitckaia, A. Poulesquen, Design of lightweight metakaolin based geopolymer foamed with hydrogen peroxide, Ceram. Int. 45 (2019) 1322–1330. doi:10.1016/j.ceramint.2018.10.021.

[77] H. Gonçalves, B. Gonçalves, L. Silva, N. Vieira, F. Raupp-Pereira, L. Senff, J.A. Labrincha, The influence of porogene additives on the properties of mortars used to control the ambient moisture, Energy Build. 74 (2014) 61–68. doi:10.1016/j.enbuild.2014.01.016.

[78] L. Senff, G. Ascensão, D. Hotza, V.M. Ferreira, J.A. Labrincha, Assessment of the single and combined effect of superabsorbent particles and porogenic agents in nanotitania-containing mortars, Energy Build. 127 (2016) 980–990. doi:10.1016/j.enbuild.2016.06.048.

[79] L. Senff, R.C.E. Modolo, G. Ascensão, D. Hotza, J.A. Labrincha, V.M. Ferreira, Development of mortars containing superabsorbent polymer, Constr. Build. Mater. 95 (2015) 575–584. doi:10.1016/j.conbuildmat.2015.07.173.

[80] H. Gonçalves, B. Gonçalves, L. Senff, L. Silva, F. Raupp-Pereira, J.A. Labrincha, Development of porogene-containing mortars for levelling the indoor ambient moisture, Ceram. Int. 40 (2014) 15489–15495. doi:10.1016/j.ceramint.2014.07.010.

[81] L. Senff, G. Ascensão, V.M. Ferreira, M.P. Seabra, J.A. Labrincha, Development of multifunctional plaster using nano-TiO2and distinct particle size cellulose fibers, Energy Build. 158 (2018) 721–735. doi:10.1016/j.enbuild.2017.10.060.

[82] C. Leiva, Y. Luna-Galiano, C. Arenas, B. Alonso-Fariñas, C. Fernández-Pereira, A porous geopolymer based on aluminum-waste with acoustic properties, Waste Manag. 95 (2019) 504–512. doi:10.1016/j.wasman.2019.06.042.

[83] T.C. Hung, J.S. Huang, Y.W. Wang, K.Y. Lin, Inorganic polymeric foam as a sound absorbing and insulating material, Constr. Build. Mater. 50 (2014) 328–334. doi:10.1016/j.conbuildmat.2013.09.042.

[84] C. Arenas, Y. Luna-Galiano, C. Leiva, L.F. Vilches, F. Arroyo, R. Villegas, C. Fernández-Pereira, Development of a fly ash-based geopolymeric concrete with construction and demolition wastes as aggregates in acoustic barriers, Constr. Build. Mater. 134 (2017) 433–442. doi:10.1016/j.conbuildmat.2016.12.119.

Table 1 Apparent density of various AAM composites and foams reported in literature (grey highlighted: densities greater 700 kg/m^{3}g; orange highlighted: densities between 300 and 700 kg/m^3; green highlighted: densities below than 300 kg/m^3. For comparison purposes the aggregates (or the foaming agent) nature and amount was also included in the table.

Material	Solid precursor	Lightweight aggregate	Foaming agent	Apparent density (kg/m^3)	Reference
Polystyrene – AAM composite	Metakaolin	Polystyrene; 100 wt.% [a]	H$_2$O$_2$; 3 wt.% [a]	100	[49]
AAM foam	Coal fly ash + metakaolin	-	H$_2$O$_2$ (~4 wt.%) + foam stabilizer (~0.18 wt.%)	154	[58]
Cork – AAM composites [b]	**Biomass fly ash + metakaolin (70:30 wt.%)**	**Cork; 90 vol.%**	**-**	**168**	**This work**
AAM foam	Coal fly ash	-	H$_2$O$_2$; 4.8 wt.% [c]	239	[51]
Cork – AAM composites [b]	**Biomass fly ash + metakaolin (70:30 wt.%)**	**Cork; 87.5 vol.%**	**-**	**257**	**This work**
Cork – AAM composites	Metakaolin	Cork; 92 vol.%	-	260	[19]
AAM foam	Coal fly ash	-	H$_2$O$_2$ + foam stabilizer (1 wt.%)	310	[55]
AAM foam	Biomass fly ash + metakaolin (66.6:33.3 wt.%)	-	H$_2$O$_2$; 0.57 wt.%	390	[50]
AAM foam	Biomass fly ash + metakaolin (33.3:66.6 wt.%)	-	Al; 0.08 wt.%	430	[53]
AAM foam	Biomass fly ash + metakaolin (66.6:33.3 wt.%)	-	H$_2$O$_2$; 1.37 wt.%	440	[23]
EPS – AAM composite	Metakaolin	EPS; 72.5 vol.%	-	516	[20]
AAM foam	Biomass fly ash + metakaolin (33.3:66.6 wt.%)	-	H$_2$O$_2$; 1.2 wt.% [a]	520	[52]
AAM foam	Coal fly ash	-	H$_2$O$_2$ (1.5 wt.%) + SDS (4 wt.%)	580	[57]
AAM foam	GBFS + coal fly ash (50:50 wt.%)	-	SDS+H$_2$O$_2$	650	[56]
AAM foam	Coal fly ash + GBFS (70:30 wt.%)	-	Pre-foaming with air (16 wt.%)	720	[16]
Expanded glass – AAM composite	Coal fly ash + GGBS (70:30 wt.%)	Expanded glass	Air entrapping agent (3 L/m^3)	881	[45]
Polyurethane – AAM composite	Metakaolin	Polyurethane; 20 wt.%	-	885	[46]
AAM foam	Coal fly ash	-	Al; 0.05 wt.%	890	[54]
AAM foam	Coal fly ash	-	Diluted protein-based	940	[25]
Cenospheres – AAM composite	Coal fly ash + GBFS (21:14 wt.%)	Cenospheres; 38 wt.%	-	978	[47]
Crumb rubber – AAM composite	Coal fly ash	Crumb rubber; 96 wt.%		1067	[21]
Expanded vermiculite – AAM composite	Slag	Vermiculite	-	1918	[48]

[a] Regarding the metakaolin content; [b] The font in bold identifies the results obtained in this work; [c] Regarding the waterglass content.

GBFS – granulated blast furnace slag; GGBF - ground granulated blast furnace slag; Al – aluminium powder; SDS – sodium dodecyl sulfate

Table 2 Thermal conductivity of the AAM and the cork – AAM composite prepared with various cork amounts.

Composition	Cork (vol.%)	Thermal conductivity (mW/m K)
AAM	-	273 ± 7
Cork – AAM composites	45.0	187 ± 3
	60.0	166 ± 6
	75.0	95 ± 2
	77.5	92 ± 2
	80.0	88 ± 2
	85.0	77 ± 2
	87.5	68 ± 3